

Graph Sampling Based Deep Metric Learning for Generalizable Person Re-Identification

Shengcai Liao* and Ling Shao

Inception Institute of Artificial Intelligence (IIAI), Abu Dhabi, UAE

<https://liaosc.wordpress.com/>

Abstract

Generalizable person re-identification has recently got increasing attention due to its research values as well as practical values. However, the efficiency of learning from large-scale data has not yet been much studied. In this paper, we argue that the most popular random sampling method, the well-known PK sampler, is not informative and efficient for deep metric learning. Though online hard example mining improves the learning efficiency to some extent, the mining in mini batches after random sampling is still limited. Therefore, this inspires us that the hard example mining should be shifted backward to the data sampling stage. To address this, in this paper, we propose an efficient mini batch sampling method called Graph Sampling (GS) for large-scale metric learning. The basic idea is to build a nearest neighbor relationship graph for all classes at the beginning of each epoch. Then, each mini batch is composed of a randomly selected class and its nearest neighboring classes so as to provide informative and challenging examples for learning. Together with an adapted competitive baseline, we improve the previous state of the arts in generalizable person re-identification significantly, by up to 22.3% in Rank-1 and 15% in mAP. Besides, the proposed method also outperforms the competitive baseline by up to 4%, with the training time significantly reduced by up to $\times 6.6$, from 12.2 hours to 1.8 hours in training a large-scale dataset RandPerson with 8,000 IDs. Code is available at <https://github.com/ShengcaiLiao/QAConv>.

1. Introduction

Person re-identification aims at finding the same person of the query image from a large set of gallery images, which is a popular computer vision task. In the recent two years, generalizable person re-identification has got increasing attention due to its research values as well as practical values

[17, 6, 31, 14, 7, 12, 32, 26]. It studies the generalizability of a learned person re-identification model, and follows direct cross-dataset evaluation for performance benchmarking.

Beyond novel generalizable algorithms, a way to achieve this goal is to enlarge the scale and diversity of the training data. For example, a recent dataset called RandPerson [22] synthesized 8,000 ID and observed improved generalization ability for person re-identification. However, the efficiency of learning from large-scale data has not yet been much studied in the person re-identification community. There are two popular ways in learning deep person re-identification neural networks, namely classification based (with ID loss [28]) and metric learning based (with pairwise loss [25, 2] or triplet loss [4]), or their combinations (e.g. ID + triplet loss). With ID loss the learning is convenient for classification, however, with deep networks in large-scale learning, the learning of classifier parameters requires large memory and computation in both forward and backward passes. This is especially not easy with complex matching modules. For example, in a recent method QAConv [12] where full feature map convolution is required for matching, learning with its class memory is difficult to scale up.

Therefore, deep metric learning with only mini batches is more suited for large-scale person re-identification learning. Accordingly, the batch sampler plays an important role for efficient learning [4, 24]. The well-known PK sampler [4] is the most popular random sampling method in person re-identification. It firstly randomly selects P classes, and then randomly samples K images per class to construct a mini batch of size $B = P \times K$. Since this is performed fully randomly, the sampled instances within a mini batch may be uniformly distributed in the whole dataset (see Fig. 1 (a)), therefore, it may not be informative and efficient for person re-identification metric learning. To address this, an online hard example mining method has been proposed in [4], which improves the learning efficiency to some extent. However, the mining is performed online on the already sampled mini batches, therefore, it is still limited by the drawback of the fully random PK sampler, because the

*Corresponding Author.

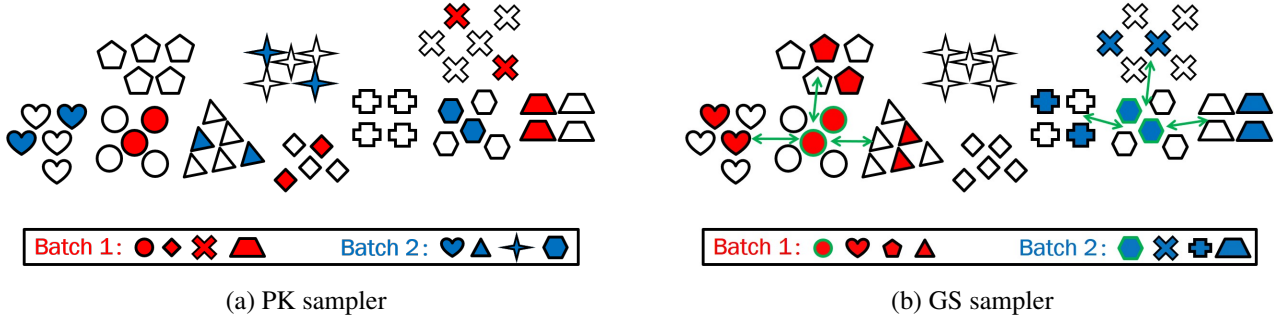


Figure 1. Two different sampling methods: (a) the PK sampler; and (b) the proposed graph sampler (GS). Shapes indicate different classes while colors indicate different batches. GS constructs a graph for all classes and always samples nearest neighboring classes.

mini batches obtained by the PK sampler do not consider the global data distribution information.

To address this, we propose to shift backward the hard example mining to the data sampling stage. Accordingly, we propose an efficient mini batch sampling method called Graph Sampling (GS) for large-scale metric learning. The basic idea is to build a nearest neighbor relationship graph for all classes at the beginning of each epoch. Then, the mini batch sampling is performed by randomly selecting a class and its top- k nearest neighboring classes, with the same K instances per class, as shown in Fig. 1 (b). This way, instances within a sampled mini batch are mostly similar to each other, so as to provide informative and challenging examples for discriminant learning.

The contributions of this paper are summarized as follows.

- We propose a new mini batch sampling method GS, and prove that the GS sampler enables much more efficient learning than the well-known PK sampler.
- We improve a very competitive baseline by up to 4%, with the training time significantly reduced by up to $\times 6.6$, from 12.2 hours to 1.8 hours in training the large-scale dataset RandPerson with 8,000 IDs.
- Together with the baseline, we improve the previous state of the arts in generalizable person re-identification significantly, by up to 22.3% in Rank-1 and 15% in mAP.

2. Related Work

Metric learning approaches have been widely studied in the early stage of person re-identification. There are a lot of algorithms proposed, for example, the well-known PRDC [29], KISSME [8], XQDA [11], to name a few. In recent years, deep metric learning has been popular and has been extensively studied. Beyond feature representation learning, specific deep metric learning can be roughly classified into loss function designs and deep feature matching schemes. For loss function designs, pairwise loss functions

[25, 2], classification or identification loss [28], and triplet loss [4] are the most popular ones. For deep feature matching schemes, a number of methods have been proposed in the literature. For example, Ahmed et al. proposed a deep convolutional architecture with layers specially designed for local neighborhood matching [1]. Li et al. proposed a novel filter pairing neural network (FPNN) to jointly handle some known challenges in person re-identification, such as misalignment and occlusions [9]. Shen et al. proposed an end-to-end deep Kronecker-Product Matching (KPM) network [16] for softly aligned matching for person re-identification. Suh et al. proposed a deep neural network to learn part-aligned bilinear representations for person re-identification [18]. Liao and Shao proposed the Query Adaptive Convolution (QAConv) for explicit deep feature matching, and proved to be effective for generalizable person re-identification [12].

Generalizable person re-identification was initially studied in [25, 5], where direct cross-dataset evaluation was proposed to benchmark algorithms. With the advancement in deep learning, the study of generalizable person re-identification has got increasing attention in recent years. For example, Song et al. [17] proposed a domain-invariant mapping network for generalizable person re-identification, and further followed a meta-learning pipeline for effective training. Jia et al. [6] adopted both instance and feature normalization to alleviate both style and content variances across datasets to improve generalizability. Zhou et al. proposed a new backbone network, called OSNet, and showed its advantage in generalizing deep models [31]. Qian et al. proposed a leader-based multi-scale attention deep architecture (MuDeep) for person re-identification, with improved cross-dataset performance [14]. Jin et al. proposed a style normalization and restitution module for generalizable person re-identification, which shows good generalizability [7]. Yuan et al. proposed an adversarial domain-invariant feature learning network (ADIN) for generalizable person re-identification, which explicitly learns to separate identity-related features from challenging variations [26]. Zhuang et al. proposed a Camera-based Batch Nor-

malization (CBN) method for domain-invariant representation learning [32]. Though improved generalizability is obtained, unlike other methods, CBN requires additional target data to adapt the camera-based batch normalization. On the other hand, Wang et al. proposed a large-scale synthesized person re-identification dataset called RandPerson, and proved that models learned from synthesized data generalized promising to real-world datasets [22].

However, current methods are still far from satisfactory in generalization for practical person re-identification. Take face recognition as a successful example, future directions may gradually be learning from large-scale data, either supervised, semi-supervised, or unsupervised. However, the efficiency of learning from large-scale data has been little studied in person re-identification. As basic as the mini-batch sampler, though it plays an important role in deep metric learning [4, 24], it still has not yet been much studied.

3. Deep Metric Learning

There are two popular ways in learning deep person re-identification neural networks. The first one is the classification based [28], also known as the identification loss, or ID loss. This is a straightforward extension from general image classification. Since person re-identification is an open-class problem, the learned classifier is usually dropped after training. The last feature embedding layer is usually adopted instead (known as identity embedding, or IDE [28], and the Euclidean or Cosine distance is applied to measure the distance between two person images. The second one is the triplet loss based [15, 4], which is usually combined with the ID loss. Together with the online hard example mining, the triplet loss is a very useful auxiliary loss function to enhance the discriminability of the learned model.

However, the above methods always require classifier parameters, which need large memory and computation in both forward and backward passes with deep networks in large-scale learning. With dot products in classification this is still acceptable to some extent, but with more complex modules, e.g. in QAConv [12] where full feature map convolution is required for matching, learning with ID tensors is difficult to scale up.

Therefore, for large-scale deep metric learning, we consider not to use ID layers. Accordingly, pairwise verification or binary classification is another solution [25, 10]. The person re-identification method QAConv [12] is adopted as our baseline, which is the recent state of the art for generalizable person re-identification. It constructs query adaptive convolutional kernels on the fly for image matching, which suits pairwise learning. However, the original design of QAConv learning is based on the so called class memory, which stores one feature map for each class for image-to-class matching, instead of pairwise matching among mini-

batch samples. Considering the matching complexity of the QAConv layer, this is not efficient in large-scale learning. Therefore, we only consider pairwise matching among mini-batch samples for the QAConv learning, and remove its class memory module. For convenience, the resulting method is denoted by QAConv-P.

Specifically, we use the QAConv layer to compute similarity values between a pair of images, and formulate a pairwise verification or binary classification problem in mini-batch based learning. Accordingly, we compute the binary cross entropy loss as follows.

$$\ell(\theta) = -\frac{1}{B} \sum_{i=1}^B \sum_{j \neq i} y_{ij} \log(p_{ij}(\theta)) + (1-y_{ij}) \log(1-p_{ij}(\theta)), \quad (1)$$

where B is the mini-batch size, θ is the network parameter, $p_{ij} \in [0, 1]$ is the QAConv similarity indicating binary classification probability, and $y_{ij} = 1$ indicates a positive pair, while a negative pair otherwise.

4. Graph Sampling

4.1. Motivation

It is proved in [12] that the learning with class memory is more effective than triplet loss among mini-batch samples. This is reasonable because it is popular that the well known PK sampler [4] is used to provide mini-batch samples for the optimization of the triplet loss, but its random nature in sampling instances is not informative enough for discriminant learning. In the PK sampler, as shown in Fig. 1 (a), P classes and K images per class are randomly sampled for each mini batch. Though an online hard example mining (OHEM) is further proposed in [4] to find informative instances within a mini batch for learning, the PK sampler itself is still not efficient, which provides limited hard examples for OHEM to mine.

Therefore, the sampling method itself needs to be improved so as to provide informative samples for each mini batch. Instead of a fully random sampling, we argue that the relationships among classes need to be considered in the sampling. Accordingly, we construct a graph for all classes at the beginning of each epoch, and always samples nearest neighboring classes in a mini batch so as to challenge the discriminant learning. We call this idea Graph Sampling (GS), which is introduced in detail in the following subsection.

4.2. GS Sampler

To enable informative sampling, at the beginning of each epoch, we utilize the currently learned model to evaluate distances or similarities between classes, and then construct a graph for all classes, so that the relationships among classes can be used for effective sampling. Specifically, we

randomly select one image per class to construct a small sub-dataset. Then, feature embeddings of the current network are extracted, denoted as $\mathbf{X} \in R^{C \times d}$, where C is the total number of classes for training, and d is the feature dimension. Next, the current distance function (if parameterized) is used to calculate pairwise distances among all the selected samples. In our experiments, we use the QAconv [12] method to calculate the distances. As a result, a distance matrix $dist \in R^{C \times C}$ among all classes is obtained. To improve the distance measure, we further apply the re-ranking technique [30] on the resulting distance matrix.

Then, for each class c , its top $P - 1$ nearest neighboring classes can be retrieved, denoted by $\mathcal{N}(c) = \{x_i | i = 1, 2, \dots, P - 1\}$, where P is the number of classes to sample in each mini batch. Accordingly, a graph $G = (V, E)$ can be constructed, where $V = \{c | c = 1, 2, \dots, C\}$ represents the vertices, with each class being one node, and $E = \{(c_1, c_2) | c_2 \in \mathcal{N}(c_1)\}$ represents the edges.

Finally, for the mini batch sampling, for each class c , we retrieve all its connected classes in G . Then, together with c , we obtain a set $A = \{c\} \cup \{x | (c, x) \in E\}$, where $|A| = P$. Next, for each class in A , we randomly sample K instances per class to generate a mini batch of $B = P \times K$ samples.

A pseudocode of the GS sampler is shown in Algorithm 1. Note that different from other mini-batch sampling methods, for the GS sampler the number of mini batches or iterations per epoch is always C , which is independent to the parameters B , P , and K . Nevertheless, the parameter B still affects the computation load of each mini batch. Besides, one may worry that the GS sampler will be computationally expensive. However, note that firstly, only one image per class is randomly sampled for the graph construction; and secondly, the above computation is performed only once per epoch. In practice, we find that the GS sampler with QAConv, which is already a heavy matcher compared to the main-stream Euclidean distance, only requires tens of seconds for thousands of IDs. Details will be presented in Section 5.4.1.

4.3. Initialization and Gradient Clipping

Note that in the GS sampler, a properly initialized model needs to be provided for the feature extraction and distance calculation. Otherwise the constructed graph will not reflect the true relationships among classes. Besides, since the GS sampler provides almost the hardest mini batches for training, if the model is not yet properly initialized, it may suffer an optimization difficulty which may cause a problem for the model learning to converge (c.f. Section 5.4.4). In practice, we adopt the random PK sampler for the learning of the first epoch. We find that this is enough to initialize the model well. More epochs with the random PK sampler is not necessary, and may degrade the discriminability of the learned model. There will be an analysis in Section 5.4.4

Algorithm 1: Graph Sampler

Input: Data source \mathbf{D} , feature extractor \mathbf{f} , pairwise distance function \mathbf{d} , re-ranking function \mathbf{R} , batch size B , number of instances per class K .
Output: Sample iterator of the dataset \mathbf{D} .
Initialization: $pids$: list of all class IDs;
 $index_dict$: dictionary of list containing all sample indices of each class.
Procedure:
 $index = []$
for p in $pids$:
 $index.append(\text{random.choice}(index_dict[p], \text{size}=1))$ # randomly select one sample per class
 $dataset = \mathbf{D}(index)$ # construct a small sub-dataset
 $X = \mathbf{f}(dataset)$ # extract features
 $dist = \mathbf{d}(X, X)$ # calculate pairwise distance
 $dist = \mathbf{R}(dist)$ # re-rank the dist
 $dist[i, i] = \text{Inf}$ # ignore the diagonal elements
 $P = B / K$ # number of classes in a mini batch
 $topk_index = \text{topk}(-dist, \text{size}=P-1)$ # find nearest neighboring classes
 $index = []$
for p in $\text{shuffle}(pids)$:
 $index.extend(\text{random.choice}(index_dict[p], \text{size}=K))$ # randomly select K samples per class
 for k in $topk_index[p]$:
 $index.extend(\text{random.choice}(index_dict[k], \text{size}=K))$ # randomly select K samples per class
Return: $\text{iter}(index)$

regarding this.

Furthermore, also because the GS sampler provides almost the hardest mini batches for training, the gradients may explode during training, especially in the initial stage. Therefore, to stable the training with the GS sampler, we clip the gradient norm during the backward propagation. Specifically, let \mathbf{g} be the gradient of all parameters, and $\|\mathbf{g}\|$ be its norm. Then the gradient will be clipped as $\mathbf{g} \leftarrow \min(1, \frac{T}{\|\mathbf{g}\|}) \cdot \mathbf{g}$, where T is a predefined threshold. The effect of this gradient clipping will be analyzed in Section 5.4.5.

5. Experiments

5.1. Implementation Details

Our implementation is adapted from the official PyTorch code of QAConv¹ [12]. We first build an improved baseline based on QAConv, with most settings being the same with the authors' updated code. Specifically, the ResNet-50 [3] is used as the backbone network, with Instance Normaliza-

¹<https://github.com/ShengcaiLiao/QAConv>

tion (IN) [20] layer appended to the last block of layer1 and layer2, according to several recent studies [13, 6, 31, 7, 32]. The layer3 feature map is used, with a neck convolution of 64 channels appended as the final feature map. The input image size is 384×128 . Several commonly used data augmentation methods are applied, including random cropping, flipping, occlusion, and color jittering. The batch size is set to 8. The SGD optimizer is adopted to train the network, with a learning rate of 0.0005 for the backbone network, and 0.005 for newly added layers. They are decayed by 0.1 after 10 epochs, and the training stops at 15 epochs, except that on RandPerson the total number of epochs is 4, and the learning rate step size is 2, according to the official code and the experience in [22].

As for the proposed method QAConv-P, the only difference to the above baseline is the loss computation and the data sampler. We use the proposed GS sampler, with $B=64$, and $K=4$. Besides, we use a smaller learning rate of 0.001.

5.2. Datasets

Four large-scale person re-identification datasets, CUHK03 [9], Market-1501 [27], MSMT17 [23], and RandPerson [22] were used in our experiments. The CUHK03 dataset contains 1,360 persons and 13,164 images. The more challenging detected subset was used for experiments. Besides, the CUHK03-NP protocol [30] was adopted, with 767 and 700 subjects used for training and test, respectively. The Market-1501 dataset includes 32,668 images of 1501 identities captured from 6 cameras. The training subset contains 12,936 images from 751 identities, while the test subset includes 19,732 images from 750 identities for testing. The MSMT17 dataset contains 4,101 identities and 126,441 images captured from 15 cameras. It is divided into a training set of 32,621 images from 1,041 identities, and a test set with the remaining images from 3,010 identities. The RandPerson dataset is a recently released synthesized person re-identification dataset. It contains 8,000 persons and 1,801,816 images. We used a subset of it, including 132,145 images of the 8,000 IDs. This dataset is only used for a large-scale training and generalization testing.

Cross-dataset evaluation was performed among these datasets, by training on the training subset of one dataset (except that in MSMT17 we further used an additional setting with all images for training), and evaluating on the test subset of another dataset. The cumulative matching characteristic (CMC) and mean Average Precision (mAP) were used as the performance evaluation metrics. All evaluations followed the single-query evaluation protocol.

5.3. Comparison to The State of The Arts

The comparison to the state of the arts (SOTA) in generalizable person re-identification is shown in Table 1, where

three datasets are used for training, while three others are used for testing. Besides, with MSMT17 as the training set, one setting is to use all images for training, regardless of its subset splits. This is denoted by MSMT17 (all). Several generalizable person re-identification methods published very recently are compared, including OSNet [31], MuDeep [14], SNR [7], QAConv [12], CBN [32], and ADIN [26]. From Table 1 it can be observed that the proposed method significantly improves the previous SOTA. For example, with Market-1501 \rightarrow CUHK03-NP, the Rank-1 and mAP are improved by 6.1% and 6.6%, respectively. With Market-1501 \rightarrow MSMT17, they are improved by 15.9% and 5.5%, respectively. With MSMT17 \rightarrow Market-1501, the improvements are 8.0% for Rank-1 and 12.5% for mAP. With RandPerson as the training data, the improvements on Market-1501 are 14.4% for Rank-1 and 15% for mAP, and the improvements on MSMT17 are 22.3% for Rank-1 and 8.1% for mAP. Though RandPerson is a synthesized dataset, the results show that the model learned on RandPerson generalizes quite promising on real-world datasets, which confirms the finding in [22].

Note that the major improvements come from a very competitive baseline, which is adapted from the QAConv. Note also that some methods are orthogonal to us, and their designed architectures can also be considered to improve our method. For example, OSNet [31] is proved to be a new and effective backbone. SNR [7] and CBN [32] both improve the normalization layers of a backbone network. Besides, CBN utilizes some target data to adapt the BN layer in a quick and unsupervised way.

5.4. Ablation Study

5.4.1 Comparison to the QAConv baseline

Table 1 also shows the comparison between the proposed QAConv-P + GS and the competitive baseline QAConv we adapted. From the results shown in Table 1 it can be observed that, beyond the successful learning scheme of the class memory proposed in QAConv, the proposed QAConv-P metric learning with the GS sampler is also very effective in learning discriminant models. QAConv-P + GS outperforms QAConv for all experiments, with up to 4.4% improvements.

Furthermore, we also compare the training time of QAConv (with the class memory) and QAConv-P + GS. Both methods are tested on a single NVIDIA V100 GPU. From the comparison shown in Table 1 it can be observed that the original QAConv learned with class memory becomes very slow when trained with large-scale dataset, such as the full MSMT17 and the RandPerson datasets. This is not surprising because in each mini-batch iteration QAConv needs to compute matching scores between mini-batch samples and the feature map memory of all classes, while the number of classes in MSMT17 is 4,101, and it is 8,000 in RandPer-

Table 1. Comparison of the state-of-the-art direct cross-dataset evaluation results (%). MSMT17 (all) means all images are used for training, regardless of subset splits.

Method	Venue	Training		CUHK03-NP		Market-1501		MSMT17	
		Data	Time (h)	Rank-1	mAP	Rank-1	mAP	Rank-1	mAP
MGN [21, 14]	ACMMM 2018	Market-1501	-	8.5	7.4	-	-	-	-
MuDeep [14]	TPAMI 2020	Market-1501	2	10.3	9.1	-	-	-	-
CBN [32]	ECCV 2020	Market-1501	-	-	-	-	-	25.3	9.5
QAConv [12]	ECCV 2020	Market-1501	-	9.9	8.6	-	-	22.6	7.0
QAConv	Baseline	Market-1501	1.07	13.3	14.2	-	-	40.9	14.7
QAConv-P + GS	Ours	Market-1501	0.68	16.4	15.7	-	-	41.2	15.0
PCB [19, 26]	ECCV 2018	MSMT17	-	-	-	52.7	26.7	-	-
MGN [21, 26]	ACMMM 2018	MSMT17	-	-	-	48.7	25.1	-	-
ADIN [26]	WACV 2020	MSMT17	-	-	-	59.1	30.3	-	-
SNR [7]	CVPR 2020	MSMT17	-	-	-	70.1	41.4	-	-
CBN [32]	ECCV 2020	MSMT17	-	-	-	73.7	45.0	-	-
QAConv	Baseline	MSMT17	2.37	15.6	16.2	72.9	44.2	-	-
QAConv-P + GS	Ours	MSMT17	0.96	20.0	19.2	75.1	46.7	-	-
OSNet [31]	CVPR 2019	MSMT17 (all)	-	-	-	66.5	37.2	-	-
QAConv [12]	ECCV 2020	MSMT17 (all)	-	25.3	22.6	72.6	43.1	-	-
QAConv	Baseline	MSMT17 (all)	17.85	25.1	24.8	79.5	52.3	-	-
QAConv-P + GS	Ours	MSMT17 (all)	3.88	27.2	27.1	80.6	55.6	-	-
RP Baseline [22]	ACMMM 2020	RandPerson	-	13.4	10.8	55.6	28.8	20.1	6.3
QAConv	Baseline	RandPerson	12.22	12.6	12.1	73.2	42.1	41.8	13.8
QAConv-P + GS	Ours	RandPerson	1.84	14.8	13.4	74.0	43.8	42.4	14.4

son. In contrast, the proposed pairwise learning with the GS sampler is much more efficient because it avoids matching all classes for each iteration. As can be seen from Table 1, the training time of the baseline QAConv can be significantly reduced by up to $\times 6.6$, which can be considered a significant achievement of this competitive baseline.

On the other hand, we also evaluate the sampling efficiency of the proposed GS sampler. As stated earlier, it constructs a graph at the beginning of each epoch. We evaluate the running time of all the computations in Algorithm 1. The results are 4 seconds on Market-1501, 9 seconds on MSMT17 training subset, 40 seconds on the full MSMT17 dataset, and 138 seconds on RandPerson with 8,000 IDs. Therefore, the GS sampler is in fact efficient, though with QAConv, which is already a heavy matcher compared to the main-stream Euclidean distance.

5.4.2 Learning efficiency

Next, we compare the learning efficiency of three methods: QAConv with class memory, QAConv-P + PK sampler, and QAConv-P + GS sampler, as shown in Fig. 2. Comparing QAConv-P + GS to QAConv-P + PK, it can be observed that with the GS sampler the learning is much more efficient, especially with large epochs. This is because the GS sampler always provides the most informative mini batches for training. Besides, this result also confirms that the ran-

dom PK sampler is inefficient for deep metric learning.

Comparing QAConv-P + GS to the class memory based QAConv, it can be observed from Fig. 2 that both methods learn effectively. However, though it seems that QAConv with class memory learns more effectively at the beginning, it turns out that QAConv-P + GS is superior in the later learning stage, thanks to the GS sampler which generates hard examples in mini batches to challenge the learning.

5.4.3 Parameter analysis

In Fig. 3, we show the performance with different parameter configurations of the GS sampler, trained on Market-1501. We observe that for the batch size, generally the accuracy increases with the increasing batch size (thus increasing P), but saturates at about 64. It is understood that mini batches with larger batch size provides more comprehensive data for learning, however, at the cost of enlarged computation time, recalling that the number of iterations per epoch is fixed as C for the GS sampler. For example, with $B = 64$, the training of QAConv-P + GS on Market-1501 is about 0.68 hours on a single V100 GPU. However, this is about 1.32 hours with $B = 128$ for training the same epochs.

Next, we evaluate the influence of K under fixed $B = 64$, as shown in Fig. 3 (b). Interestingly, larger K leads to gradually better performance on the CUHK03-NP, however, it degrades the performance significantly on MSMT17. It

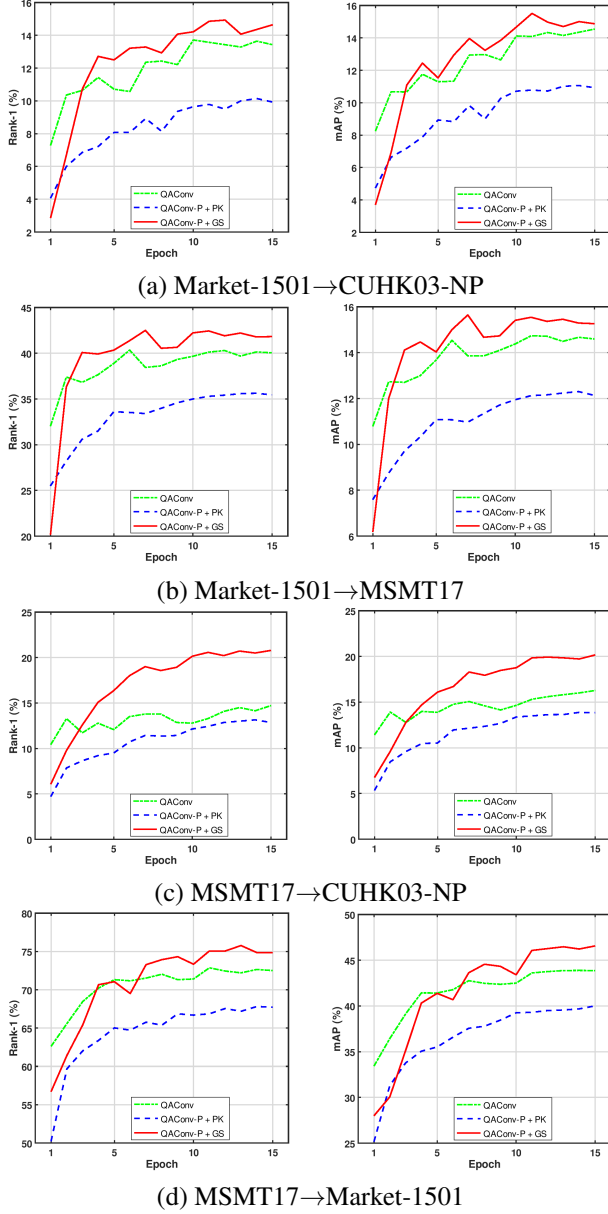


Figure 2. Learning efficiency of three methods (QAConv with class memory, QAConv-P + PK sampler, and QAConv-P + GS sampler) w.r.t the number of epochs.

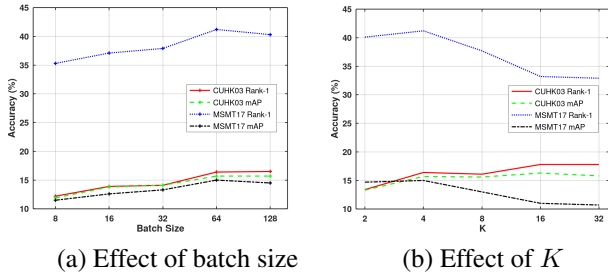


Figure 3. Performance with different parameter configurations of the GS sampler, trained on Market-1501. (a) with varying batch size under fixed $K = 4$; and (b) with varying K under fixed $B = 64$.

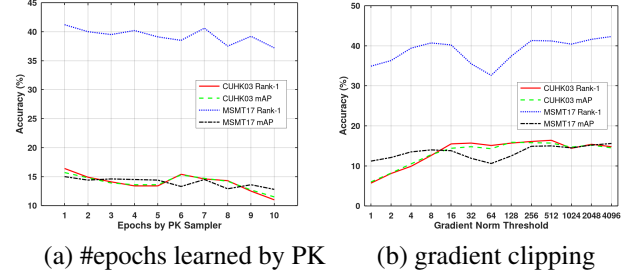


Figure 4. Influence of initialization and gradient clipping trained on Market-1501. (a) Performance of different number of early epochs adopting the PK sampler. (b) Performance of different gradient clipping thresholds.

appears that $K = 4$ is a reasonable trade-off.

5.4.4 Effect of initialization

To understand how to initialize the model learning for QAConv-P + GS, we assign different number of early epochs among the total 15 epochs to the PK sampler, and report the results, which are trained on Market-1501, in Fig. 4 (a). Note that with no epochs learned by the random PK sampler, that is, the GS sampler starts from the very beginning, the model cannot converge. Thus this result is not shown in Fig. 4 (a). As the performance shown in Fig. 4 (a), it can be observed that generally the performance degrades with the increasing number of epochs learned by the PK sampler. This is because the PK sampler provides limited informative examples for learning, and hence it should be replaced by the GS sampler as early as possible, as long as the model can normally learn. Therefore, we find that one epoch for the PK sampler initialization is enough.

5.4.5 Effect of gradient clipping

Next, we study the effect of the gradient clipping to the learning of QAConv-P + GS. The results trained on Market-1501 is shown in Fig. 4 (b). One can see that generally the performance increases with the increasing value of the gradient clipping threshold, but saturates or slightly degrades after 512. This is understood that small threshold values limit the model to learn effectively, and hence degrade the discriminability of the learned model. However, some information is not revealed in Fig. 4 (b). With large threshold values, it is quite often that the model learning cannot converge, due to the gradient exploding problem, because the GS sampler is too aggressive. We need to run several times for large threshold values to get the results. Therefore, a reasonable value of 512 is suggested for a trade-off.

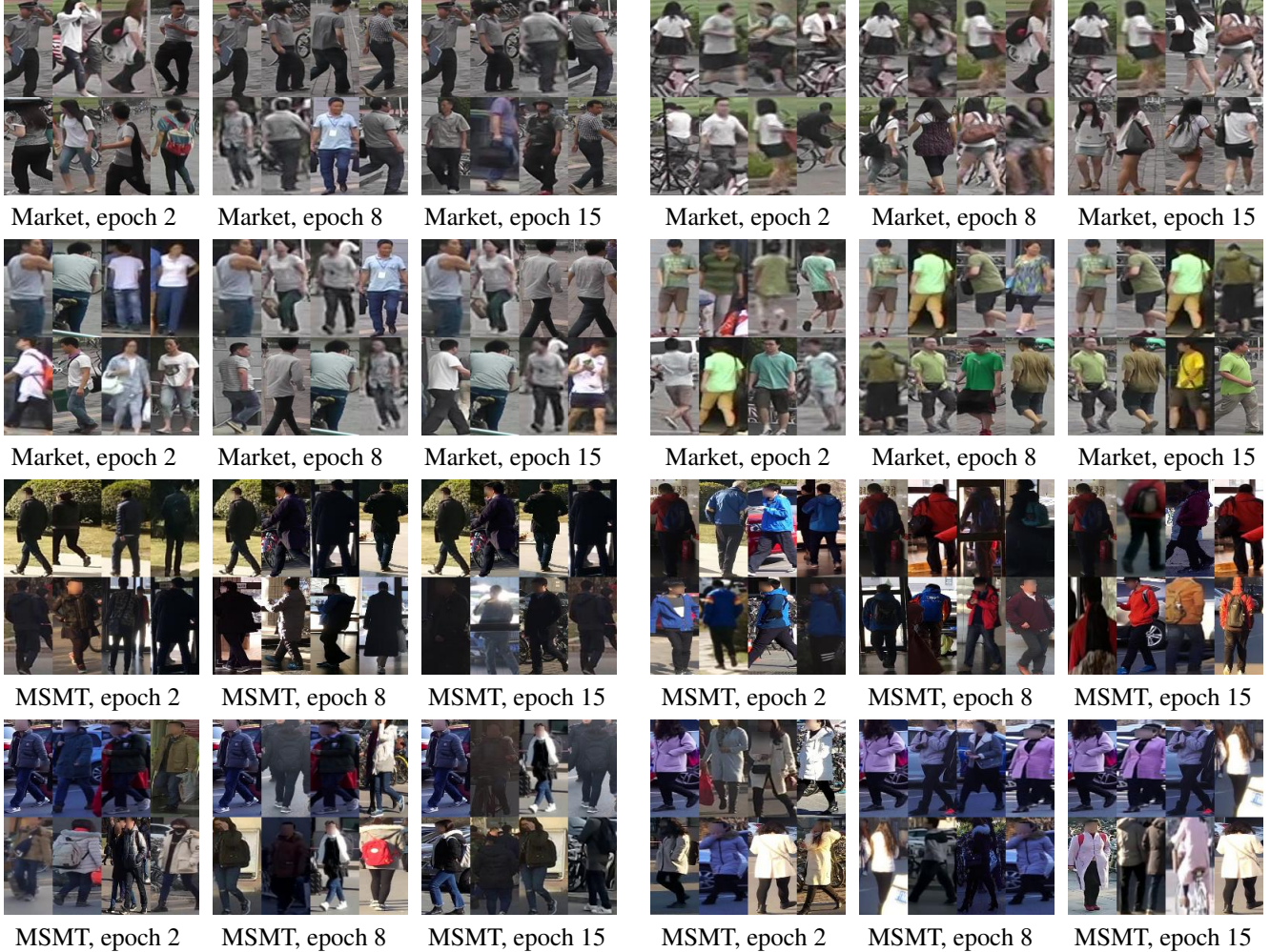


Figure 5. Eight groups of examples for the nearest neighboring classes generated by the GS sampler. The first two rows are from the training on Market-1501, while the last two rows are from that of MSMT17. In each group, three sets of images are shown, corresponding to epoch 2, 8, and 15. In each set, the upper left image is the center class, and other images are the top-7 nearest neighboring classes to the center class.

5.4.6 Visualization of GS

Finally, we show some examples for the nearest neighboring classes generated by the GS sampler in Fig. 5. It can be observed that, the GS sampler is indeed able to find similar classes as hard examples to challenge the learning. Besides, it seems that in early epochs, the model tends to evaluate similarity with visual appearance, regardless of foreground and background. However, in late epochs, the model learns to remove the influence of background, and learns higher level of abstraction.

6. Conclusion

With this study, we demonstrate that the popular PK sampler is not efficient in deep metric learning, and a new batch sampler called Graph Sampler helps to learn discriminant models more efficiently. This is achieved by con-

structing a nearest neighbor graph of all classes for informative sampling. Together with a competitive baseline, we achieve the new state of the art in generalizable person re-identification with a significant improvement. Meanwhile, the training time is much reduced by removing classification parameters and only using pairwise distances among mini batches for loss computation. We believe the proposed technique is general and may also be applied in other fields, such as image retrieval, face recognition, among others.

References

- [1] Ejaz Ahmed, Michael Jones, and Tim K Marks. An improved deep learning architecture for person re-identification. In *Proceedings of the IEEE Conference on Computer Vision and Pattern Recognition*, pages 3908–3916, 2015. 2
- [2] Weijian Deng, Liang Zheng, Qixiang Ye, Guoliang Kang, Yi Yang, and Jianbin Jiao. Image-Image Domain Adaptation

- with Preserved Self-Similarity and Domain-Dissimilarity for Person Re-identification. In *Proceedings of the IEEE Computer Society Conference on Computer Vision and Pattern Recognition*, 2018. 1, 2
- [3] K. He, X. Zhang, S. Ren, and J. Sun. Deep residual learning for image recognition. In *Proceedings of IEEE Computer Society Conference on Computer Vision and Pattern Recognition*, pages 770–778, 2016. 4
- [4] Alexander Hermans, Lucas Beyer, and Bastian Leibe. In defense of the triplet loss for person re-identification, 2017. 1, 2, 3
- [5] Yang Hu, Dong Yi, Shengcai Liao, Zhen Lei, and Stan Z. Li. Cross dataset person Re-identification. In *ACCV Workshop on Human Identification for Surveillance (HIS)*, pages 650–664, 2014. 2
- [6] Jieru Jia, Qiuqi Ruan, and Timothy M Hospedales. Frustratingly easy person re-identification: Generalizing person re-id in practice. In *British Machine Vision Conference*, 2019. 1, 2, 5
- [7] Xin Jin, Cuiling Lan, Wenjun Zeng, Zhibo Chen, and Li Zhang. Style Normalization and Restitution for Generalizable Person Re-identification. In *CVPR*, feb 2020. 1, 2, 5, 6
- [8] M Kostinger, Martin Hirzer, Paul Wohlhart, Peter M Roth, and Horst Bischof. Large scale metric learning from equivalence constraints. In *IEEE Conference on Computer Vision and Pattern Recognition*, 2012. 2
- [9] Wei Li, Rui Zhao, Tong Xiao, and Xiaogang Wang. Deep-ReID: Deep filter pairing neural network for person re-identification. In *IEEE Conference on Computer Vision and Pattern Recognition*, 2014. 2, 5
- [10] Wei Li, Rui Zhao, Tong Xiao, and Xiaogang Wang. Deep-reid: Deep filter pairing neural network for person re-identification. In *Proceedings of IEEE Computer Society Conference on Computer Vision and Pattern Recognition*, 2014. 3
- [11] Shengcai Liao, Yang Hu, Xiangyu Zhu, and Stan Z. Li. Person re-identification by local maximal occurrence representation and metric learning. In *IEEE Conference on Computer Vision and Pattern Recognition*, 2015. 2
- [12] Shengcai Liao and Ling Shao. Interpretable and Generalizable Person Re-Identification with Query-Adaptive Convolution and Temporal Lifting. In *European Conference on Computer Vision (ECCV)*, 2020. 1, 2, 3, 4, 5, 6
- [13] Xingang Pan, Ping Luo, Jianping Shi, and Xiaoou Tang. Two at once: Enhancing learning and generalization capacities via ibn-net. In *Proceedings of the European Conference on Computer Vision (ECCV)*, pages 464–479, 2018. 5
- [14] Xuelin Qian, Yanwei Fu, Tao Xiang, Yu-Gang Jiang, and Xiangyang Xue. Leader-based Multi-Scale Attention Deep Architecture for Person Re-identification. *TPAMI*, 2020. 1, 2, 5, 6
- [15] Florian Schroff, Dmitry Kalenichenko, and James Philbin. FaceNet: A unified embedding for face recognition and clustering. In *Proceedings of the IEEE Computer Society Conference on Computer Vision and Pattern Recognition*, 2015. 3
- [16] Yantao Shen, Tong Xiao, Hongsheng Li, Shuai Yi, and Xiaogang Wang. End-to-end deep kronecker-product matching for person re-identification. In *Proceedings of the IEEE Conference on Computer Vision and Pattern Recognition*, pages 6886–6895, 2018. 2
- [17] Jifei Song, Yongxin Yang, Yi-Zhe Song, Tao Xiang, and Timothy M Hospedales. Generalizable person re-identification by domain-invariant mapping network. In *Proceedings of the IEEE Conference on Computer Vision and Pattern Recognition*, pages 719–728, 2019. 1, 2
- [18] Yumin Suh, Jingdong Wang, Siyu Tang, Tao Mei, and Kyoung Mu Lee. Part-aligned bilinear representations for person re-identification. *Proceedings of the European Conference on Computer Vision (ECCV)*, pages 402–419, 2018. 2
- [19] Yifan Sun, Liang Zheng, Yi Yang, Qi Tian, and Shengjin Wang. Beyond part models: Person retrieval with refined part pooling (and a strong convolutional baseline). In *Proceedings of the European Conference on Computer Vision (ECCV)*, 2018. 6
- [20] Dmitry Ulyanov, Andrea Vedaldi, and Victor Lempitsky. Improved texture networks: Maximizing quality and diversity in feed-forward stylization and texture synthesis. In *Proceedings - 30th IEEE Conference on Computer Vision and Pattern Recognition, CVPR 2017*, 2017. 5
- [21] Guanshuo Wang, Yufeng Yuan, Xiong Chen, Jiwei Li, and Xi Zhou. Learning discriminative features with multiple granularities for person re-identification. In *2018 ACM Multimedia Conference on Multimedia Conference*, pages 274–282. ACM, 2018. 6
- [22] Yanan Wang, Shengcai Liao, and Ling Shao. Surpassing Real-World Source Training Data: Random 3D Characters for Generalizable Person Re-Identification. In *28th ACM International Conference on Multimedia (ACMMM)*, 2020. 1, 3, 5, 6
- [23] Longhui Wei, Shiliang Zhang, Wen Gao, and Qi Tian. Person transfer gan to bridge domain gap for person re-identification. In *Proceedings of the IEEE Conference on Computer Vision and Pattern Recognition*, pages 79–88, 2018. 5
- [24] Mang Ye, Jianbing Shen, Gaojie Lin, Tao Xiang, Ling Shao, and Steven C. H. Hoi. Deep Learning for Person Re-identification: A Survey and Outlook. *arXiv preprint arXiv:2001.04193*, 2020. 1, 3
- [25] Dong Yi, Zhen Lei, Shengcai Liao, and Stan Z. Li. Deep metric learning for person re-identification. In *International Conference on Pattern Recognition*, pages 34–39, Dec. 2014. 1, 2, 3
- [26] Ye Yuan, Wuyang Chen, Tianlong Chen, Yang Yang, Zhou Ren, Zhangyang Wang, and Gang Hua. Calibrated Domain-Invariant Learning for Highly Generalizable Large Scale Re-Identification. *WACV*, pages 3578–3587, nov 2020. 1, 2, 5, 6
- [27] L. Zheng, L. Shen, L. Tian, S. Wang, J. Wang, and Q. Tian. Scalable person re-identification: A benchmark. In *Proceedings of IEEE International Conference on Computer Vision*, 2015. 5
- [28] Liang Zheng, Hengheng Zhang, Shaoyan Sun, Manmohan Chandraker, Yi Yang, and Qi Tian. Person re-identification

- in the Wild. In *Proceedings - 30th IEEE Conference on Computer Vision and Pattern Recognition, CVPR 2017*, 2017. 1, 2, 3
- [29] Wei-Shi Zheng, Shaogang Gong, and Tao Xiang. Person re-identification by probabilistic relative distance comparison. In *Proceedings of IEEE Computer Society Conference on Computer Vision and Pattern Recognition*, pages 649–656, 2011. 2
- [30] Zhun Zhong, Liang Zheng, Donglin Cao, and Shaozi Li. Re-ranking person re-identification with k-reciprocal encoding. In *Proceedings of the IEEE Conference on Computer Vision and Pattern Recognition*, pages 1318–1327, 2017. 4, 5
- [31] Kaiyang Zhou, Yongxin Yang, Andrea Cavallaro, and Tao Xiang. Omni-scale feature learning for person re-identification. In *Proceedings of the IEEE International Conference on Computer Vision*, 2019. 1, 2, 5, 6
- [32] Zijie Zhuang, Longhui Wei, Lingxi Xie, Tianyu Zhang, Hengheng Zhang, Haozhe Wu, Haizhou Ai, and Qi Tian. Rethinking the Distribution Gap of Person Re-identification with Camera-based Batch Normalization. In *ECCV*, pages 140–157, jan 2020. 1, 3, 5, 6